

DOI: 10.1002/chem.201302567

1,2,4-Triazol-3-ylidenes with an *N*-2,4-Dinitrophenyl Substituent as Strongly π -Accepting N-Heterocyclic Carbenes

Tetsuo Sato,^{*,[a, b]} Yoichi Hirose,^[a] Daisuke Yoshioka,^[a] Tsubasa Shimojo,^[a] and Shuichi Oi^{*,[a, b]}

Abstract: The synthesis and characterization of a series of new Rh and Au complexes bearing 1,2,4-triazol-3-ylidenes with a *N*-2,4-dinitrophenyl (*N*-DNP) substituent are described. IR, NMR, single-crystal X-ray diffraction and computational analyses of the Rh complexes revealed that the N-heterocyclic carbenes (NHCs) behaved as strong π acceptors and weak σ donors.

In particular, a natural bond orbital (NBO) analysis revealed that the contributions of the Rh \rightarrow C_{carbene} π back-bonding interaction energies (ΔE_{bb}) to the bond dissociation energies (BDE)

of the Rh–C_{carbene} bond for [RhCl(NHC)(cod)] (cod=1,5-cyclooctadiene) reached up to 63%. The Au complex exhibited superior catalytic activity in the intermolecular hydroalkoxylation of cyclohexene with 2-methoxyethanol. The NBO analysis suggested that the high catalytic activity of the Au^I complex resulted from the enhanced π acidity of the Au atom.

Keywords: acidity • carbene ligands • gold • ligand effects • rhodium

Introduction

There has been great interest in N-heterocyclic carbenes (NHCs) as ligands for transition metal complex catalysts and organocatalysts because of the high flexibility in the molecular design of their electronic and structural properties.^[1] Although research on metal NHC complexes has focused primarily on their excellent carbene carbon-to-metal σ -donating properties, which make the metal atom highly nucleophilic, some electron-deficient NHCs, which were shown to be weak σ donors from the IR spectra of [RhCl(NHC)(CO)₂], have been developed in the last decade (Figure 1).^[2] Experimental investigations and theoretical studies on this new class of NHCs have revealed improved metal-to-carbene carbon π -accepting abilities. Electron-deficient NHCs have been prepared by various methods, such as modification of the backbone (**A**),^[2e,f] using electron-withdrawing *N* substituents (**IDNP** and **C**),^[3] and incorporation of electronegative heteroelements in the basic framework of imidazol-2-ylidenes (**B** and **D**). Furthermore, various 1,2,4-triazol-3-ylidenes have been synthesised.^[1n-r,2m-o,4] However, there have been very few reports on the effects of π -accept-

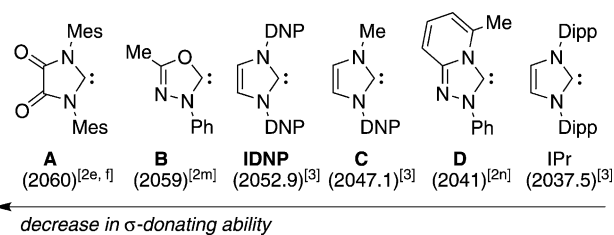


Figure 1. Comparison of σ -donating abilities of selected NHCs. The average IR stretching frequencies $\tilde{\nu}_{av}(\text{CO})$ [cm^{-1}] of CO in [RhCl(NHC)(CO)₂] are shown in parentheses. IR spectra were recorded in CH₂Cl₂ for **A**, **C**, **IDNP**, and **IPr**, in KBr for **B**, and as a film for **D**. DNP = 2,4-dinitrophenyl. Dipp = 2,6-diisopropylphenyl.

ing NHC ligands on transition-metal catalysis.^[2p,4e-g,5] Moreover, most ligands studied, such as **D**,^[5] have stronger σ -donating than π -accepting capabilities. Recently, we synthesised *N*-2,4-dinitrophenyl (DNP)-substituted imidazol-2-ylidenes **IDNP** and **C**, and showed that the DNP group effectively increased the π -accepting abilities of carbenes.^[3] Here we report the synthesis of a series of Rh^I and Au^I complexes of 1,2,4-triazol-3-ylidenes bearing the *N*-DNP substituent and evaluate the electronic properties of these NHCs through experimental and theoretical analyses.

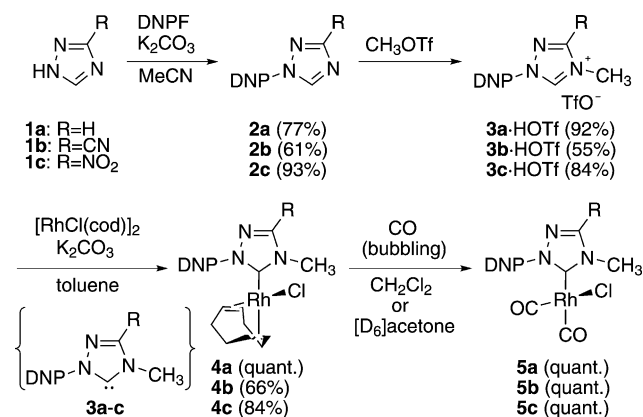
Results and Discussion

Synthesis of Rh^I and Au^I complexes: To compare the differences in the electronic properties of the carbenes, we chose three triazoles **1a–c** as the starting materials, substituted with an H, cyano, or nitro group at the 5-position (Scheme 1). 2,4-Dinitrophenylation of **1a–c** afforded **2a–c**, and subsequent methylation with an excess of methyl triflate

[a] Dr. T. Sato, Y. Hirose, D. Yoshioka, T. Shimojo, Prof. Dr. S. Oi
Department of Applied Chemistry
Graduate School of Engineering, Tohoku University
6-6-11 Aramaki-Aoba, Aoba-ku, Sendai 980-8579 (Japan)
Fax: (+81)22-795-5874
E-mail: tetsuo@aporg.che.tohoku.ac.jp
oishu@aporg.che.tohoku.ac.jp

[b] Dr. T. Sato, Prof. Dr. S. Oi
Environment Conservation Research Institute, Tohoku University
6-6-11 Aramaki-Aoba, Aoba-ku, Sendai 980-8579 (Japan)

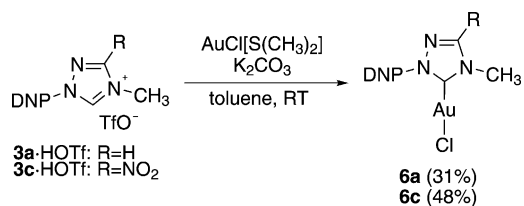
Supporting information for this article is available on the WWW under <http://dx.doi.org/10.1002/chem.201302567>.



Scheme 1. Synthesis of Rh^I complexes **4a–c** and **5a–c**.

provided triazolium salts **3a–c**·HOTf, the structures of which were confirmed by NMR spectroscopy, elemental analysis, and single crystal X-ray diffraction.^[6] The generation of carbenes and complexation was then examined. Although the free NHCs **3a–c** could not be isolated, treatment of triazolium salts **3a–c**·HOTf with $[\{\text{RhCl}(\text{cod})\}_2]$ (cod = 1,5-cyclooctadiene) in the presence of K₂CO₃ as base in toluene at room temperature afforded the corresponding $[\text{RhCl}(\text{NHC})(\text{cod})]$ (**4a–c**) in good yields through in situ generation of NHCs **3a–c**, respectively. To estimate the σ -donating properties of NHCs **3a–c**, Rh complexes **4a–c** were converted to $[\text{RhCl}(\text{NHC})(\text{CO})_2]$ (**5a–c**) in quantitative yield by bubbling CO gas through their solutions in CH₂Cl₂ or [D₆]acetone. $[\text{RhCl}(\text{IPr})(\text{cod})]$ (**4e**)^[7] and $[\text{RhCl}(\text{IPr})(\text{CO})_2]$ (**5e**)^[8] were also prepared for comparison of the electronic properties of the NHCs. In addition, $[\text{AuCl}(\text{NHC})]$ complexes **6a** and **6c** were synthesised by the reactions of triazolium salts **3a**·HOTf or **3c**·HOTf with AuCl(SMe₂) and K₂CO₃ as base (Scheme 2). The structures of the Rh^I complexes **4a–c** and Au^I complexes **6a** and **6c** were determined by NMR spectroscopy, elemental analysis, and single-crystal X-ray diffraction.

Characterisation of $[\text{RhCl}(\text{NHC})(\text{CO})_2]$ (5**):** First, we characterised the electronic properties of the new NHCs **3a–c** by performing IR and ¹³C NMR spectroscopic analyses of Rh^I complexes **5a–c**. They were compared to the corresponding Rh^I complexes bearing imidazol-2-ylidene analogues such as **C** and IPr. The Tolman electronic parameters (TEP)^[9] of **3a–c**, determined from the averages of the IR CO stretching frequencies $\tilde{\nu}_{\text{av}}(\text{CO})$ of Rh^I dicarbonyl complexes **5a–c**,^[1b,10] were significantly higher compared to that



Scheme 2. Synthesis of Au^I complexes **6a** and **6c**.

Table 1. Summary of the IR and ¹³C NMR spectroscopic analyses of $[\text{RhCl}(\text{L})(\text{CO})_2]$ (**5a–e**).

Complex	$\tilde{\nu}(\text{CO})$ ^[a]	$\tilde{\nu}_{\text{av}}(\text{CO})$ ^[b]	TEP ^[c]	$\delta(^{13}\text{C}_{\text{N}_2})$ ^[d]
5a (L= 3a)	2093.4, 2015.3	2054.4	2064	182.7
5b (L= 3b)	2099.1, 2021.0	2060.1	2068	186.9
5c (L= 3c)	2100.1, 2022.0	2061.1	2069	190.6
5d (L= C)	2086.6, 2007.5 ^[3]	2047.1 ^[3]	2058	–
5e (L=IPr)	2078.9, 1996.0 ^[3]	2037.5 ^[3]	2050	179.8

[a] IR CO stretching frequencies [cm⁻¹] in CH₂Cl₂. [b] Average of $\tilde{\nu}(\text{CO})$ [cm⁻¹]. [c] Tolman electronic parameter (TEP) [cm⁻¹] calculated with the equation $\text{TEP} = 0.8001\tilde{\nu}_{\text{av}}(\text{CO}) + 420.0$.^[1b] [d] ¹³C NMR chemical shift [ppm] of the carbenic carbon atom in [D₆]acetone.

of IPr, calculated from $\tilde{\nu}_{\text{av}}(\text{CO})$ of **5e**. Thus, **3a–c** exhibit extremely poor σ -donating properties (Table 1). Since the TEP value of **3a** (2064 cm⁻¹) was larger than that of **C** (2058 cm⁻¹), it appears that the incorporation of the N atom into the NHC framework reduced the σ -donating ability of the NHC. Notably, the TEP values of **3c** and **3b** (2069 and 2068 cm⁻¹, respectively) are the highest reported so far, even higher than those of **A**^[2e,f] and **B**^[2m] (Figure 1). In this work, as the TEP value increased, we observed a downfield shift in the ¹³C NMR signal of the carbenic carbon atom in the Rh^I dicarbonyl complexes (Table 1).^[11] These results suggest that an increase in the deshielding of the carbon atom corresponds to a decrease in its σ -donating ability.

Characterisation of $[\text{RhCl}(\text{NHC})(\text{cod})]$ (4**):** Next, we characterised the Rh^I complexes **4a–c** by performing crystallographic, ¹³C NMR spectroscopic, and theoretical analyses. Figures 2–4 show ORTEPs of **4a–c**, respectively. Single crystals for X-ray diffraction analysis were obtained by slow cooling of a hot CH₃CN solution of **4a** and slow diffusion of diethyl ether into CH₂Cl₂ solutions of **4b** and **4c**. All com-

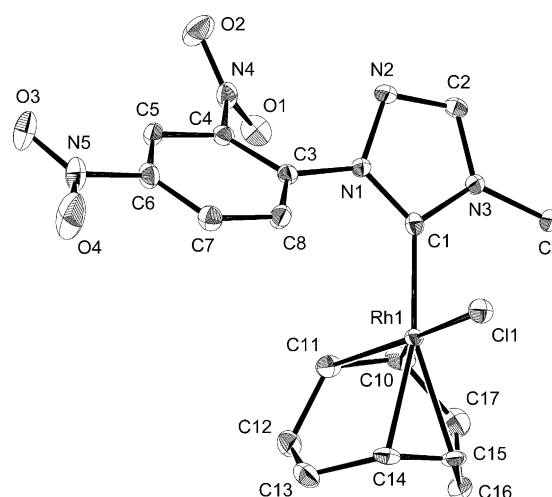


Figure 2. ORTEP of **4a** with thermal ellipsoids at 50% probability. Hydrogen atoms and an acetonitrile solvent molecule have been omitted for clarity. Selected distances [Å] and angles [°]: Rh1–C1 2.003(3), Rh1–C10 2.112(3), Rh1–C11 2.131(3), Rh1–C14 2.218(2), Rh1–C15 2.209(3), Rh1–C11 2.3776(7), C1–N1 1.356(3), C1–N3 1.359(3); N1–C1–N3 102.0(2), C1–Rh1–C11 88.22(8), N1–C1–Rh1–C11 –98.1(2), C1–N1–C3–C4 –141.7(3), C3–C4–N4–O1 46.4(3), C5–C6–N5–O3 –6.2(4).

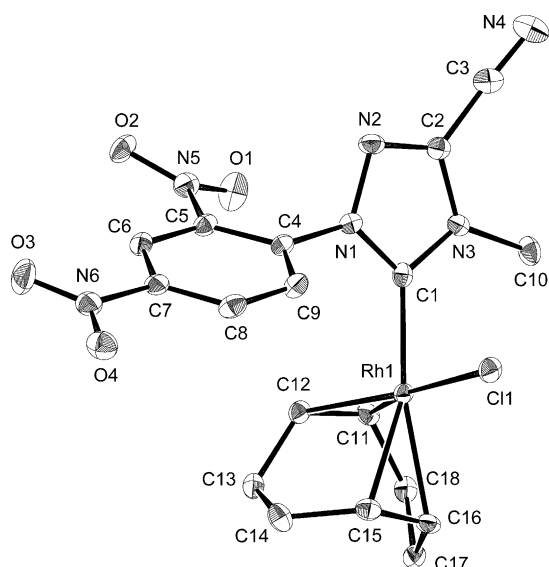


Figure 3. ORTEP of **4b** with thermal ellipsoids at 50% probability. Hydrogen atoms have been omitted for clarity. Selected distances [Å] and angles [°]: Rh1–C1 1.993(2), Rh1–C11 2.119(2), Rh1–C12 2.140(2), Rh1–C15 2.199(2), Rh1–C16 2.226(2), Rh1–C11 2.3808(7), C1–N1 1.351(3), C1–N3 1.358(3); N1–C1–N3 102.1(2), C1–Rh1–Cl1 85.04(7), Cl1–Rh1–C1–N1 –90.9(2), C1–N1–C4–C5 –118.9(3), O1–N5–C5–C4 22.9(3), O3–N6–C7–C6 –6.0(3).

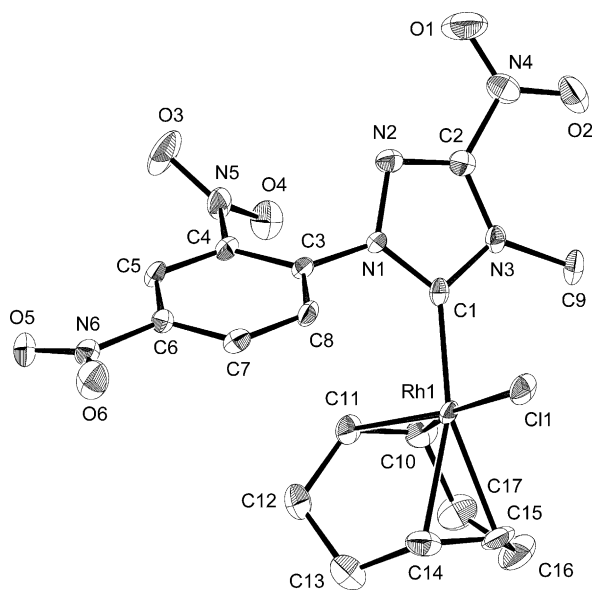


Figure 4. ORTEP of **4c** with thermal ellipsoids at 50% probability. Hydrogen atoms have been omitted for clarity. Selected distances [Å] and angles [°]: Rh1–C1 1.989(2), Rh1–C10 2.124(3), Rh1–C11 2.119(2), Rh1–C14 2.230(3), Rh1–C15 2.218(2), Rh1–C11 2.3801(7), C1–N1 1.350(3), C1–N3 1.362(3); N1–C1–N3 102.7(2), C1–Rh1–Cl1 87.68(7), Cl1–Rh1–C1–N1 –98.9(2), O1–N4–C2–N2 –3.3(4), C1–N1–C3–C4 –128.3(2), O3–N5–C4–C3 39.4(3), O5–N6–C6–C5 15.1(3).

plexes have pseudo-square-planar metal centres coordinated by NHC ligands **3a**, **3b**, or **3c**, a chloride anion, and COD ligand. The dihedral angles between the NHC framework and the metal–ligand plane are approximately orthogonal (–98.1(2)° for **4a**, –90.9(2)° for **4b**, and –98.9(2)° for **4c**).

In all complexes, the NHC frameworks scarcely conjugate with the DNP group in the solid-state structure, and this indicates that the DNP group acts as an electron-withdrawing group through an inductive effect. The dihedral angles between the NHC and DNP frameworks are –141.7(3)° for **4a**, –118.9(3)° for **4b**, and –128.3(2)° for **4c**. However, the NHC framework is on almost the same plane as the nitro group at the 5-position in complex **4c** (O1–N4–C2–N2 –3.3(4)°). As expected from the TEP values of **3a–c**, **C**, and IPr, the Rh–C_{carbene} crystallographic distance in the Rh^I complexes **4a–e** (Table 2) decrease in the order **4e**

Table 2. Summary of the crystallographic and ¹³C NMR spectroscopic analyses of RhCl(L)(cod) **4a–e**.

Complex	Rh–C _{carbene} [a]	% V _{bur} [b]	δ(¹³ CN ₂) [c]	δ(<i>trans</i> - ¹³ CH _{COD}) [d]
4a (L= 3a)	2.003(3)	29.0	190.3	99.5, 99.3
4b (L= 3b)	1.993(2)	28.7	194.2	100.9, 100.7
4c (L= 3c)	1.989(2)	29.6	198.1	101.3, 101.1
4d (L= C)	2.017(2) ^[3]	29.4 ^[3]	184.1 ^[3]	97.8, 97.4 ^[3]
4e (L=IPr)	2.054(4) ^[12]	34.0 ^[12]	183.6 ^[3]	93.9 ^[3]

[a] The crystallographic distance [Å] between the Rh atom and the carbene carbon atom. [b] The % V_{bur} values were calculated with the Bondi radii scaled by 1.17, a sphere of radius 3.5 Å, a mesh size of 0.05 Å, and an Rh–NHC distance of 2.00 Å with omission of all hydrogen atoms. [c] ¹³C NMR chemical shift [ppm] of the carbene carbon atom in [D₆]DMSO. [d] ¹³C NMR chemical shift [ppm] of the alkene moiety of COD *trans* to the ligand (L) in [D₆]DMSO.

(2.054(4) Å^[12]), **4d** (2.017(2) Å^[3]), **4a** (2.003(3) Å), **4b** (1.993(2) Å), and **4c** (1.989(2) Å). There is not much difference in the steric bulk of the NHCs **3a**, **3b**, **3c**, and **C** in their respective complexes **4a–d**. The percent buried volume (% V_{bur}) values were estimated to be 29.0, 28.7, 29.6, and 29.4%,^[3] respectively (Table 2).^[13] Furthermore, the ¹³C NMR chemical shifts of both of the carbene carbon atom and the alkene moiety of COD *trans* to the NHC ligand of **4a–e** shifted to the downfield with decreasing σ-donating ability of the ligands, which is in agreement with previous results (Table 2).^[2b,14] These results indicate that the π-accepting abilities of the NHC ligands increased in the order of **4e**, **4d**, **4a**, **4b**, and **4c**.

Theoretical analysis of [RhCl(NHC)(cod)] (4): To evaluate the electronic properties of the NHC ligands for **4a–e**, we performed a natural bond orbital (NBO) analysis (Table 3). The calculation showed that the natural atomic charges δ of the carbene carbon atoms in **4a–e** increased positively corresponding to a downfield shift of the ¹³C NMR signals, and carbene carbon atom in **4c** had the most positive charge. The Wiberg bond indexes *W* between the Rh atom and the carbene carbon atom in **4a–e** increased with decreasing Rh–C_{carbene} crystallographic distance. In addition, an NBO second-order perturbation analysis revealed that the increase in the π backbonding interaction energies (Δ*E*_{bb}) was accompanied by a decrease in the Rh–C_{carbene} bond length and an increase in the TEP value. The Δ*E*_{bb} value of **4a** with triazol-3-ylidene **3a** (27.64 kcal mol^{–1}) is larger than that of **4d** bearing imidazol-2-ylidene analogue **C** (24.68 kcal

Table 3. Summary of the computational analysis of [RhCl(L)(cod)] (**4a–e**).

Complex	$\delta_{\text{C}}^{[a]}$	$W_{\text{RhC}}^{[b]}$	BDE ^[c]	$\Delta E_{\text{bb}}^{[d]}$	ΔE_{bb} in BDE ^[e]
4a (L= 3a)	0.400	0.723	50.40	27.64	54.8
4b (L= 3b)	0.407	0.728	48.93	30.86	63.1
4c (L= 3c)	0.416	0.737	49.15	30.92	62.9
4d (L= C)	0.402	0.709	51.95	24.68	47.5
4e (L=IPr)	0.370	0.662	53.90	20.08	37.3

[a] Natural atomic charge δ of the carbenic carbon atom. [b] Wiberg bond index W between the Rh atom and the carbenic carbon atom in the NHC ligand. [c] Bond dissociation energy [kcal mol⁻¹]. [d] π backbonding interaction energy [kcal mol⁻¹]. [e] Percentage contribution of ΔE_{bb} to BDE.

mol⁻¹). Furthermore, the nitro and cyano substituents on the NHC framework effectively enhanced the π backbonding interactions. As a result, the ΔE_{bb} values of **4b** and **4c** (30.86 and 30.92 kcal mol⁻¹, respectively) were about 12% larger than that of **4a**. Consequently, the contribution of ΔE_{bb} to the bond dissociation energy (BDE) of the Rh–C_{carbene} bond for **4b** and **4c** was 63%, whereas that for **4e** was 37%. Interestingly, the BDE did not decrease considerably, even though the electron-donating ability of the coordinated NHC decreased. This suggests that π backdonation of the NHC compensated for the decrease in σ -donation.

Energies of the σ -donor and π -acceptor orbitals of NHCs:

The energies of the σ -donor orbital (E_{σ}) and π -acceptor orbital (E_{π}) for **3a–c**, **C**, and IPr were calculated to evaluate their σ -donating and π -accepting abilities. The σ -donor orbital is an occupied carbene lone pair and the π -accepting orbital is a vacant p orbital on the carbene carbon atom (Table 4). The calculations support the above results. Substi-

Table 4. Energies of the σ -donor orbital (E_{σ}) and π -acceptor orbital (E_{π}) for NHCs **3a–c**, **C**, and IPr.

NHC	E_{σ} [eV]	E_{π} [eV]
3a	–8.70 (HOMO–7)	–2.15 (LUMO+2)
3b	–9.14 (HOMO–10)	–2.63 (LUMO+2)
3c	–9.24 (HOMO–12)	–2.71 (LUMO+3)
C ^[3]	–8.30 (HOMO–4)	–1.86 (LUMO+2)
IPr ^[3]	–7.64 (HOMO–8)	–1.38 (LUMO)

tution of the NHC framework with a cyano or nitro group in decreased both the E_{σ} and the E_{π} values. The E_{σ} values decreased from –8.70 eV in **3a** to –9.14 and –9.24 eV in **3b** and **3c**, respectively. The E_{π} values decrease from –2.15 eV in **3a** to –2.63 and –2.71 eV in **3b** and **3c**, respectively. As is evident from the substantial decrease in the values of both of E_{σ} and E_{π} , the σ -donating abilities of *N*-DNP-substituted triazol-3-ylidenes **3a–c** significantly deteriorated, whereas the π -accepting capabilities improved, compared to **C** and IPr.

Characterisation of [AuCl(NHC)] (6**):** Figures 5 and 6 show ORTEPs of **6a** and **6c**, respectively. Single crystals for X-ray diffraction analysis were obtained by slowly cooling acetone solutions of **6a** and **6c**. The Au–C_{carbene} bond length in

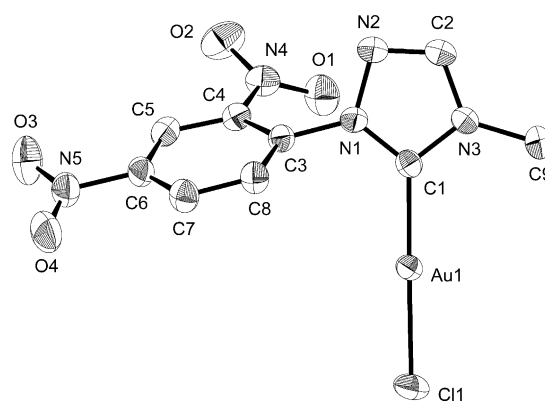


Figure 5. ORTEP of **6a** with thermal ellipsoids at 50% probability. Hydrogen atoms and an acetone solvent molecule have been omitted for clarity. Selected distances [Å] and angles [°]: Au1–C1 1.976(3), Au1–Cl1 2.2741(8), C1–N1 1.339(3), C1–N3 1.348(3); N1–C1–N3 103.5(2), C1–Au1–Cl1 177.45(7), C1–N1–C3–C4 121.4(3), O1–N4–C4–C3 –30.7(4), O3–N5–C6–C5 9.9(4).

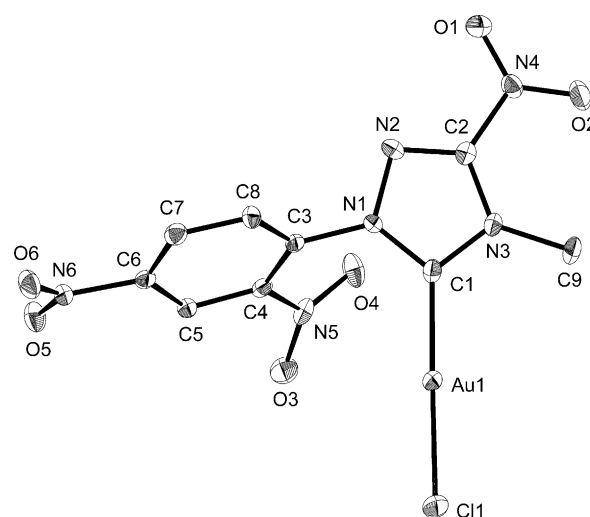


Figure 6. ORTEP of **6c** with thermal ellipsoids at 50% probability. Hydrogen atoms have been omitted for clarity. Selected distances [Å] and angles [°]: Au1–C1 1.966(4), Au1–Cl1 2.2665(12), C1–N1 1.352(5), C1–N3 1.433(5); N1–C1–N3 103.5(4), C1–Au1–Cl1 177.88(13), O1–N4–C2–N2 1.0(6), C1–N1–C3–C4 –64.7(6), O3–N5–C4–C3 152.9(4), O5–N6–C6–C5 –16.1(5).

6c (1.966(4) Å) is shorter than that in **6a** (1.976(3) Å). As with the Rh^I complexes **4a** and **4c**, the NHC frameworks scarcely conjugate with the DNP group, but are on the same plane as the nitro group at the 5-position in complex **6c**. The C1–N1–C3–C4 dihedral angles are 121.4(3)° for **6a** and –64.7(6)° for **6c**, and the O1–N4–C2–N2 dihedral angle of **6c** is 1.0(6)°.

Au-catalysed hydroalkoxylation of alkenes: We investigated the new π -accepting NHCs as ligands for π -acidic Au catalysts. It was demonstrated recently that **IDNP** is a more effective ligand than IPr and PPh₃ in Au-catalysed hydroalkoxylation of cyclohexene with 2-ethoxyethanol.^[3,15] Electronic activation of the alkene to form the alkyl Au inter-

mediate is believed to be the rate-determining step in this reaction. Since electron-deficient ligands accelerate the overall rate of a reaction,^[16] we evaluated the catalytic activity of the new Au^I complexes in the intermolecular hydroalkoxylation of alkenes. To elucidate the difference in the catalytic activities, we first chose a combination of cyclohexene (**7**) and 2-ethoxyethanol (**8**), which has also been examined previously. The results of the hydroalkoxylation of **8** with **7** are summarised in Table 5. Under optimised reaction conditions (see Supporting Information, Table S2), the catalytic

Table 5. Au-catalysed hydroalkoxylation of cyclohexene (**8**) with 2-methoxyethanol (**7**).^[a]

Entry	Au complex	T [°C]	Conversion [%] ^[b]	Yield [%] ^[b]
1	[AuCl(3c)] (6c)	100	95	81
2	[AuCl(3a)] (6a)	100	93	74
3	[AuCl(IDNP)]	100	83	66
4	[AuCl(IMes)]	100	75	59
5	[AuCl(IPr)]	100	20	7
6	[AuCl(PPh ₃)]	100	77	63
7	[AuCl{P(OPh) ₃ }	100	93	71
8	none	100	15	0

[a] Reactions were carried out with **7** (0.25 mmol), **8** (2.5 mmol), Au complex (0.0125 mmol), and AgNTf₂ (0.0125 mmol) in PhCl (0.25 mL) for 20 h. [b] Conversions and yields were determined by GLC analysis.

activities of the Au^I complexes bearing NHC ligands, PPh₃, and P(OPh)₃ were compared. The combination of **6c**, which contains the weakest σ -donating NHC **3c**, and AgNTf₂ afforded adduct **9** in the highest yield (Table 5, entry 1); **9** was formed in 81 % yield with 95 % conversion of **7** by using ten equivalents of cyclohexene with 5 mol% **6c**/AgNTf₂ in chlorobenzene at 100 °C for 20 h. The yields of the target adduct **9** followed a similar order to the TEP values (Table 5, entries 1–5). The Au^I complex bearing PPh₃ gave adduct **9** in moderate yield and conversion (Table 5, entry 6). It is known that P(OPh)₃ is more electron-deficient ligand than PPh₃; their TEP values are 2085.3 and 2068.9 cm⁻¹, respectively.^[9] Moreover, it was reported that the initial turnover frequency for addition of methanol to propyne catalysed by the Au^I complex bearing P(OPh)₃ was 2.46 times higher than that of the reaction with the Au^I-PPh₃ complex.^[17] In the hydroalkoxylation of **8** with **7** using [AuCl{P(OPh)₃}] (**9**) was only obtained in 71 % yield, al-

though the conversion of **7** reached 93 % (Table 5, entry 7). When the Au^I complex was not added, the intermolecular hydroalkoxylation did not proceed at all (Table 5, entry 8). In all cases, by-products derived from **7** were not detected by GC-MS analysis. To examine in more detail the catalytic properties of the Au^I complexes we performed the reactions at 90 °C (see Supporting Information, Table S2). The yields decreased in all reactions, but a similar trend of catalytic activities to when the reactions were carried out at 100 °C was obtained. A conversion versus time plot for the addition of **7** to **8** at 100 °C with various Au^I precatalysts is shown in Figure 7. With increasing TEP value of the NHC ligand (IPr < **IDNP** < **6a** < **6c**), the reaction rate increased. Although the initial rate of reaction with the Au^I-P(OPh)₃ complex was slightly faster than that with the Au^I-**6c** complex, the Au^I-**6c** complex afforded **9** in 10% higher yield than the Au^I-P(OPh)₃ complex under the optimised reaction conditions (Table 5, entries 1 and 7).

Theoretical analysis of Au^I complexes: To understand the difference between the intermolecular hydroalkoxylation of the alkenes catalysed by Au^I complexes bearing π -accepting NHC **3c** and σ -donating imidazol-2-ylidenes on an electronic level, we carried out an NBO analysis of Au(NHC)-(ethylene) cationic complexes **10a** and **10b**, which are model complexes of plausible intermediates. The results are summarised in Table 6.^[18] The calculation of Au→C_{carbene} and Au→ethylene π backbonding interaction energies for **10a** (coordinated by **3a**) and **10b** (bearing an imidazol-2-ylidene analogue) revealed that the same d orbital of Au was involved in the π backbonding interactions in both complexes. The Au→C_{carbene} interaction of **10a** (9.57 kcal mol⁻¹) was larger than that of **10b** (8.68 kcal mol⁻¹). In conjunction with this interaction, the magnitude of the Au→ethylene π backbonding interactions of **10a** and **10b** were reversed (24.08 and 27.13 kcal mol⁻¹, respectively), and the average natural atomic charge δ_{av} on the carbon atoms of ethylene in **10a** was more positive than that in **10b**. This indicates

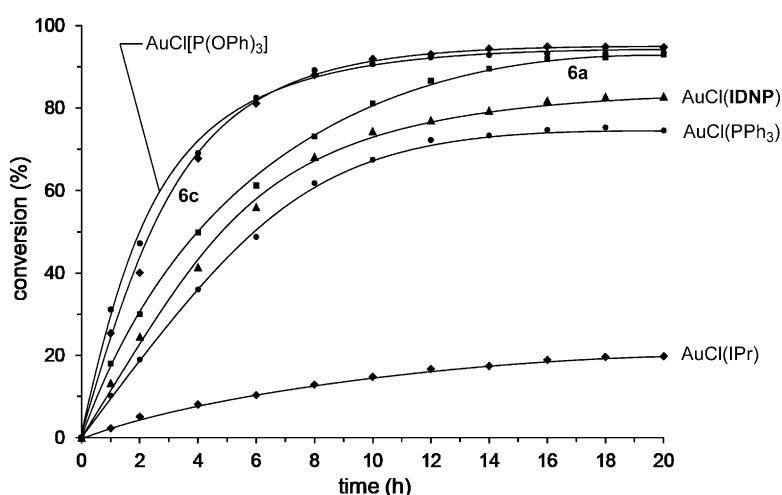
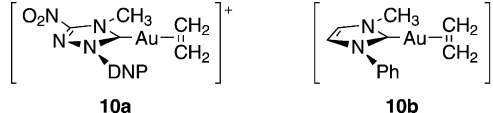


Figure 7. Time course of Au-catalysed hydroalkoxylation of cyclohexene **8** with 2-methoxyethanol **7**. Reactions were carried out with **7** (0.50 mmol), **8** (5.0 mmol), Au complex (0.025 mmol), and AgNTf₂ (0.025 mmol) in PhCl (0.5 mL) at 100 °C for 20 h. Conversions were determined by GLC analysis.

Table 6. NBO analysis of $[\text{Au}(\text{NHC})(\text{ethylene})]^+$ (**10a** and **10b**)


Complex	$\Delta E_{\text{bb}}(\text{Au} \rightarrow \text{NHC})^{[a]}$	$\Delta E_{\text{bb}}(\text{Au} \rightarrow \text{ethylene})^{[b]}$	$\delta_{\text{av}}(\text{CH}_2)^{[c]}$
10a	9.57	24.08	-0.395
10b	8.68	27.13	-0.403

[a] π backbonding interaction energy [kcal mol^{-1}] between the Au atom and the carbenic carbon atom. [b] π backbonding interaction energy [kcal mol^{-1}] between the Au atom and ethylene. [c] Average of the natural atomic charges δ on the carbon atoms in ethylene.

that **3c** enhances the π acidity of an Au atom owing to its π -accepting ability. Hence, it seems that **10a** is more favourable for the nucleophilic attack of alcohols.

Conclusion

We have synthesised a series of Rh^I complexes bearing novel *N*-DNP-substituted 1,2,4-triazol-3-ylidenes **3a–c**. The characterisation of the Rh^I complexes by spectroscopic, crystallographic, and theoretical analyses revealed that NHC **3c** with a nitro group on the NHC framework exhibited notably strong π -accepting and weak σ -donating properties. In addition, we conclude that the Au^I complex **6c** bearing the strongly π -accepting NHC **3c** is a superior precatalyst in the hydroalkoxylation of cyclohexene with 2-methoxyethanol on the basis of the yields of adducts, the conversion of alcohol, and reaction rates. An NBO analysis suggested that the high catalytic activity of the Au^I complex bearing **3c** was due to the enhanced π acidity of the Au atom resulting from remarkably large π backdonation of **3c**.

Experimental Section

General information: All reactions were carried out under an N_2 atmosphere by using a standard vacuum line, Schlenk tube techniques, and dried and deoxygenated solvents. ^1H (400.03 MHz) and ^{13}C (100.60 MHz) NMR spectra were recorded on a Bruker BioSpin AV400 NMR spectrometer. The ^1H NMR chemical shifts are given in parts per million (ppm) relative to tetramethylsilane at ($\delta = 0.00$ ppm). The $^{13}\text{C}\{^1\text{H}\}$ NMR spectra reported in ppm relative to the chemical shifts of residual undeuterated solvent signals for CDCl_3 at 77.00 ppm, $[\text{D}_6]\text{acetone}$ at 29.84 ppm (CD_3), and $[\text{D}_6]\text{DMSO}$ at 39.52 ppm. High-resolution mass spectra were obtained on a JEOL JMS-700 spectrometer at the Department of Instrumental Analysis of the Technical Division, School of Engineering, Tohoku University and a Bruker Daltonics solariX 9.4T at the Research and Analytical Center for Giant Molecules, Graduate School of Science, Tohoku University. IR spectra were recorded on a JASCO FT/IR-350 Fourier-transform infrared spectrophotometer. X-ray analysis was carried out on a Bruker AXS APEX II CCD diffractometer. GLC yields were determined on a Shimadzu GC-2010 with a GL Sciences InertCap 5MS/Sil column (L: 30 m \times i.d.: 0.25 mm, $d_i = 0.25 \mu\text{m}$) equipped with a flame ionization detector and *n*-tetradecane as internal standard. GC-MS analysis was performed on a Shimadzu PARVUM2. Preparative fractionations were performed on a Shimadzu GC-8A with a packed column (20% SE-

30 on Uniport B 60/80 mesh, L: 3 m \times i.d.: 3 mm) equipped with a thermal conductivity detector.

1-(2,4-Dinitrophenyl)-1,2,4-triazole (2a):^[19] A Schlenk flask (50 mL) was charged with 1*H*-1,2,4-triazole (**1a**, 207 mg, 3.00 mmol), K_2CO_3 (622 mg, 4.50 mmol), 1-fluoro-2,4-dinitrobenzene (558 mg, 3.00 mmol), and dry CH_3CN (5 mL). The mixture was stirred at 60 °C for 3 h. Then, the resulting salt and excess K_2CO_3 were filtered off, and the filtrate was concentrated under reduced pressure. Water (10 mL) was added to the resulting oil, and the obtained precipitate was collected by filtration. The solid was washed with water (3 \times 5 mL) and dried under vacuum to give **2a** as a yellow-green powder (540 mg, 2.30 mmol, 77%). ^1H NMR (400.03 MHz, $[\text{D}_6]\text{DMSO}$): $\delta = 9.33$ (s, 1H; ArNCHN), 8.95 (d, $^4J = 2.5$ Hz, 1H; $\text{CH}_{3\text{-Ar}}$), 8.72 (dd, $^3J = 8.8$, $^4J = 2.5$ Hz, 1H; $\text{CH}_{5\text{-Ar}}$), 8.37 (s, 1H; ArNNCHN), 8.25 ppm (d, 1H, $^3J = 8.8$ Hz; $\text{CH}_{6\text{-Ar}}$); $^{13}\text{C}\{^1\text{H}\}$ NMR (100.60 MHz, $[\text{D}_6]\text{DMSO}$): $\delta = 153.6$, 146.9, 145.5, 143.0, 133.2, 128.5, 127.4, 121.3 ppm; IR (KBr): $\tilde{\nu} = 3126.0$, 3082.7, 3061.4, 1610.3, 1546.6, 1346.1, 1030.8, 978.7, 918.9, 881.3, 853.4, 833.1, 743.4 cm^{-1} .

3-Cyano-1-(2,4-dinitrophenyl)-1,2,4-triazole (2b): A Schlenk flask (50 mL) was charged with 3-cyano-1*H*-1,2,4-triazole (**1b**, 282 mg, 3.00 mmol), K_2CO_3 (622 mg, 4.50 mmol), 1-fluoro-2,4-dinitrobenzene (558 mg, 3.00 mmol), and dry CH_3CN (5 mL). The mixture was stirred at 60 °C for 4 h. Then, the resulting salt and excess K_2CO_3 were filtered off, and the filtrate was concentrated under reduced pressure. CH_2Cl_2 (15 mL) was added to the resulting solid, and the insoluble solid was filtered off. The filtrate was concentrated under reduced pressure to give **2b** as an orange powder (473 mg, 1.82 mmol, 61%). M.p. 106–107 °C; ^1H NMR (400.03 MHz, $[\text{D}_6]\text{acetone}$): $\delta = 9.40$ (s, 1H; NCHN), 9.05 (d, $^4J = 2.5$ Hz, 1H; $\text{CH}_{3\text{-Ar}}$), 8.88 (dd, $^3J = 8.8$, $^4J = 2.5$ Hz, 1H; $\text{CH}_{5\text{-Ar}}$), 8.40 ppm (d, $^3J = 8.8$ Hz, 1H; $\text{CH}_{6\text{-Ar}}$); $^{13}\text{C}\{^1\text{H}\}$ NMR (100.60 MHz, $[\text{D}_6]\text{acetone}$): $\delta = 162.0$, 149.5, 148.4, 141.4, 134.0, 130.5, 129.8, 122.5, 112.2 ppm; IR (KBr): $\tilde{\nu} = 3129.9$, 2260.2, 1611.2, 1542.8, 1507.1, 1345.1, 1316.2, 1087.7, 983.5, 912.2, 741.5 cm^{-1} ; HRMS (EI): m/z calcd for $\text{C}_9\text{H}_4\text{N}_6\text{O}_4^+$: 260.0294 [M^+]; found: 260.0294.

1-(2,4-Dinitrophenyl)-3-nitro-1,2,4-triazole (2c):^[20] A Schlenk flask (50 mL) was charged with 3-nitro-1*H*-1,2,4-triazole (**1c**, 570 mg, 5.00 mmol), K_2CO_3 (1037 mg, 7.50 mmol), 1-fluoro-2,4-dinitrobenzene (931 mg, 5.00 mmol), and dry CH_3CN (10 mL). The mixture was stirred at 60 °C for 6 h. Then, the resulting salt and excess K_2CO_3 were filtered off, and the filtrate was concentrated under reduced pressure. CH_2Cl_2 (20 mL) was added to the resulting solid, and the insoluble solid was filtered off. The filtrate was concentrated under reduced pressure to give **2c** as a pale yellow powder (1308 mg, 4.67 mmol, 93%). M.p. 101–102 °C; ^1H NMR (400.03 MHz, $[\text{D}_6]\text{acetone}$): $\delta = 9.32$ (s, 1H; NCHN), 9.07 (d, $^4J = 2.5$ Hz, 1H; $\text{CH}_{3\text{-Ar}}$), 8.90 (dd, $^3J = 8.8$, $^4J = 2.5$ Hz, 1H; $\text{CH}_{5\text{-Ar}}$), 8.44 ppm (d, $^3J = 8.8$ Hz, 1H; $\text{CH}_{6\text{-Ar}}$); $^{13}\text{C}\{^1\text{H}\}$ NMR (100.60 MHz, $[\text{D}_6]\text{acetone}$): $\delta = 164.6$, 149.6, 148.6, 144.9, 134.1, 131.0, 130.0, 122.5 ppm; IR (KBr): $\tilde{\nu} = 1609.3$, 1560.1, 1465.6, 1432.9, 1379.8, 1335.5, 1252.5, 1141.7, 836.0, 744.4 cm^{-1} .

1-(2,4-Dinitrophenyl)-4-methyl-1,2,4-triazol-4-ium triflate (3a-HOTf): In a vial tube (5 mL), a mixture of **2a** (470 mg, 2.00 mmol) and methyl triflate (0.30 mL, 2.6 mmol) was stirred at room temperature for 15 h. To the resulting mixture, diethyl ether (3 mL) was added, and the precipitate was collected and washed with diethyl ether (2 \times 5 mL). The solid was dried under vacuum to give **3a-HOTf** as a yellow powder (733 mg, 1.84 mmol, 92%). Single crystals suitable for X-ray diffraction analysis were obtained by slow diffusion of hexane into an acetone solution of **3a-HOTf**. M.p. 189–190 °C; ^1H NMR (400.03 MHz, $[\text{D}_6]\text{DMSO}$): $\delta = 10.86$ (s, 1H; ArNCHN), 9.49 (s, 1H; ArNNCHN), 9.06 (d, $^4J = 2.4$ Hz, 1H; $\text{CH}_{3\text{-Ar}}$), 8.91 (dd, $^3J = 8.8$, $^4J = 2.4$ Hz, 1H; $\text{CH}_{5\text{-Ar}}$), 8.25 (d, $^3J = 8.8$ Hz, 1H; $\text{CH}_{6\text{-Ar}}$), 4.08 ppm (s, 3H; CH_3); $^{13}\text{C}\{^1\text{H}\}$ NMR (100.60 MHz, $[\text{D}_6]\text{DMSO}$): $\delta = 148.9$, 146.7, 145.8, 143.3, 131.3, 129.8, 129.5, 121.9, 120.7 (q, $^1J(\text{C,F}) = 322.0$ Hz), 34.9 ppm; IR (KBr): $\tilde{\nu} = 3106.8$, 3055.7, 1614, 1591.0, 1550.5, 1356.7, 1260.3, 1226.5, 1156.1, 1029.8, 637.4 cm^{-1} ; HRMS (FAB): m/z calcd for $\text{C}_9\text{H}_8\text{N}_5\text{O}_4^+$: 250.0576 [$M^+ - \text{CF}_3\text{SO}_3$]; found: 250.0576; elemental analysis calcd (%) for $\text{C}_{10}\text{H}_8\text{F}_3\text{N}_5\text{O}_7\text{S}$: C 30.08, H 2.02, N 17.54; found: C 29.98, H 2.01, N 17.45.

3-Cyano-1-(2,4-dinitrophenyl)-4-methyl-1,2,4-triazol-4-ium triflate (3b-HOTf): In a vial tube (5 mL), a mixture of **2b** (130 mg, 0.500 mmol)

and methyl triflate (1.0 mL, 9.1 mmol) was treated with ultrasonic irradiation for 1.5 h. The resulting precipitate was collected and washed with CH₂Cl₂ (2 × 3 mL). The solid was dried under vacuum to give **3b**-HOTf as an off-white powder (116 mg, 0.274 mmol, 55%). Single crystals suitable for X-ray diffraction analysis were obtained by slow cooling of a hot CH₃CN solution of **3b**-HOTf. M.p. 191–192 °C; ¹H NMR (400.03 MHz, [D₆]acetone): δ = 11.02 (s, 1H; ArNCHN), 9.19 (d, ⁴J = 2.4 Hz, 1H; CH_{3-Ar}), 9.01 (dd, ³J = 8.7, ⁴J = 2.4 Hz, 1H; CH_{3-Ar}), 8.47 (d, ³J = 8.7 Hz, 1H; CH_{6-Ar}), 4.57 ppm (s, 3H; CH₃); ¹³C{¹H} NMR (100.60 MHz, [D₆]acetone): δ = 151.1, 148.9, 144.8, 135.4, 132.7, 132.5, 130.8, 123.0, 121.9 (q, ¹J(C,F) = 322.1 Hz), 106.0, 37.2 ppm; IR (KBr): $\tilde{\nu}$ = 3098.1, 2268.8, 1544.7, 1348.0, 1284.4, 1169.6, 1028.8, 635.4 cm⁻¹; HRMS (FAB): *m/z* calcd for C₁₀H₇N₆O₄⁺: 275.0529 [*M*⁺ - CF₃SO₃]; found: 275.0532; elemental analysis calcd (%) for C₁₁H₇F₃N₆O₇S: C 31.14, H 1.66, N 19.81; found: C 30.95, H 1.69, N 19.90.

1-(2,4-Dinitrophenyl)-4-methyl-3-nitro-1,2,4-triazol-4-ium triflate (3c-HOTf): In a vial tube (5 mL), a mixture of **2c** (323 mg, 1.15 mmol) and methyl triflate (1.0 mL, 9.1 mmol) was treated with ultrasonic irradiation for 3 h. The resulting precipitate was collected and washed with CH₂Cl₂ (2 × 3 mL). The solid was dried under vacuum to give **3c**-HOTf as an orange powder (434 mg, 0.973 mmol, 84%). Single crystals suitable for X-ray diffraction analysis were obtained by the slow cooling of a hot CH₃OH solution of **3c**-HOTf. M.p. 158–159 °C; ¹H NMR (400.03 MHz, [D₆]acetone): δ = 10.96 (s, 1H; ArNCHN), 9.21 (d, ⁴J = 2.4 Hz, 1H; CH_{3-Ar}), 9.01 (dd, ³J = 8.7, ⁴J = 2.4 Hz, 1H; CH_{3-Ar}), 8.49 (d, ³J = 8.7 Hz, 1H; CH_{6-Ar}), 4.65 ppm (s, 3H; CH₃); ¹³C{¹H} NMR (100.60 MHz, [D₆]acetone): δ = 153.1, 151.2, 150.4, 144.8, 132.8, 132.4, 130.9, 123.0, 121.7 (q, ¹J(C,F) = 320.2 Hz), 39.4 ppm; IR (KBr): $\tilde{\nu}$ = 3089.4, 3014.2, 1616.1, 1573.6, 1464.7, 1350.9, 1292.1, 1252.5, 1226.5, 1150.3, 1029.8, 918.0, 841.8 cm⁻¹; HRMS (FAB): *m/z* calcd for C₉H₇N₆O₆⁺: 295.0427 [*M*⁺ - CF₃SO₃]; found: 295.0425; elemental analysis calcd (%) for C₁₀H₇F₃N₆O₉S: C 27.04, H 1.59, N 18.92; found: C 26.69, H 1.81, N 19.28.

Chloro(η⁴-cycloocta-1,5-diene)[2-(2,4-dinitrophenyl)-4-methyl-3H-1,2,4-triazol-3-ylidene]rhodium(I) (4a): A Schlenk tube (10 mL) wrapped in aluminium foil was charged with **3a**-HOTf (399 mg, 1.00 mmol), [[RhCl(cod)]₂] (247 mg, 0.500 mmol), K₂CO₃ (1.38 g, 10.0 mmol), and dry toluene (5 mL). The reaction mixture was stirred at room temperature for 3 d in the dark. After the reaction, the resulting salt and excess K₂CO₃ were filtered off, and the filtrate was concentrated under reduced pressure. The solid was dried under vacuum to give [RhCl(**3a**)(cod)] (**4a**) as an orange powder (495 mg, 0.999 mmol, 99.9%). Single crystals suitable for X-ray diffraction analysis were obtained by slow cooling of a hot CH₃CN solution of **4a**. M.p. 204 °C (decomp); ¹H NMR (400.03 MHz, [D₆]DMSO): δ = 9.34 (d, ³J = 8.6 Hz, 1H; CH_{6-Ar}), 9.00–8.93 (m, 3H; CH_{3-Ar}, CH_{5-Ar}, NCHN), 5.10–5.02 (m, 1H; CH_{COOD}), 4.96–4.87 (m, 1H; CH_{COOD}), 4.13 (s, 3H; CH₃), 3.48–3.42 (m, 1H; CH_{COOD}), 2.89–2.80 (m, 1H; CH_{COOD}), 2.44–2.26 (m, 2H; CH_{2COOD}), 2.15–2.03 (m, 1H; CH_{2COOD}), 1.96–1.78 (m, 3H; CH_{2COOD}), 1.74–1.60 ppm (m, 2H; CH_{2COOD}); ¹³C{¹H} NMR (100.60 MHz, [D₆]DMSO): δ = 190.3 (d, ¹J(Rh,C) = 50.4 Hz; NCN), 147.2, 146.5, 143.9, 136.0, 129.2, 127.6, 121.1, 99.5 (d, ¹J(Rh,C) = 7.3 Hz; CH_{COOD}), 99.3 (d, ¹J(Rh,C) = 6.2 Hz; CH_{COOD}), 69.2 (d, ¹J(Rh,C) = 14.1 Hz; CH_{COOD}), 68.8 (d, ¹J(Rh,C) = 13.7 Hz; CH_{COOD}), 35.6, 31.8, 31.6, 28.1, 27.9 ppm; IR (KBr): $\tilde{\nu}$ = 3121.2, 2987.2, 2874.4, 2825.2, 1609.3, 1543.7, 1505.2, 1425.1, 1349.0, 1262.2, 746.3 cm⁻¹; HRMS (FAB): *m/z* calcd for C₁₇H₁₉ClN₅O₄Rh⁺: 495.0181 [*M*⁺]; found: 495.0183; elemental analysis calcd (%) for C₁₇H₁₉ClN₅O₄Rh: C 41.19, H 3.86, N 14.13; found: C 40.86, H 3.96, N 14.20.

Chloro(η⁴-cycloocta-1,5-diene)[5-cyano-2-(2,4-dinitrophenyl)-4-methyl-3H-1,2,4-triazol-3-ylidene]rhodium(I) (4b): A Schlenk tube (10 mL) wrapped in aluminium foil was charged with **3b**-HOTf (106 mg, 0.250 mmol), [[RhCl(cod)]₂] (61.6 mg, 0.125 mmol), K₂CO₃ (346 g, 2.50 mmol), and dry toluene (3 mL). The reaction mixture was stirred at room temperature for 3 d in the dark. Then, the resulting salt and excess K₂CO₃ were filtered off, and the filtrate was concentrated under reduced pressure. The resulting solid was purified by column chromatography (SiO₂, CH₂Cl₂/acetone 30/1) to give [RhCl(**3b**)(cod)] (**4b**) as a brown powder (85.5 mg, 0.164 mmol, 66%). Single crystals suitable for X-ray diffraction analysis were obtained by slow diffusion of diethyl ether into

a CH₂Cl₂ solution of **4b**. M.p. 201 °C (decomp); ¹H NMR (400.03 MHz, [D₆]DMSO): δ = 9.27 (d, ³J = 9.4 Hz, 1H; CH_{6-Ar}), 9.03–8.97 (m, 2H; CH_{3-Ar}, CH_{5-Ar}), 5.12–5.04 (m, 1H; CH_{COOD}), 5.01–4.93 (m, 1H; CH_{COOD}), 4.27 (s, 3H; CH₃), 3.60–3.53 (m, 1H; CH_{COOD}), 2.92–2.85 (m, 1H; CH_{COOD}), 2.47–2.26 (m, 2H; CH_{2COOD}), 2.14–1.78 (m, 4H; CH_{2COOD}), 1.74–1.62 ppm (m, 2H; CH_{2COOD}); ¹³C{¹H} NMR (100.60 MHz, [D₆]DMSO): δ = 194.2 (d, ¹J(Rh,C) = 52.2 Hz; NCN), 147.9, 143.7, 134.9, 133.8, 129.9, 128.1, 121.5, 106.9, 100.9 (d, ¹J = 7.0 Hz; CH_{COOD}), 100.7 (d, ¹J = 6.8 Hz; CH_{COOD}), 69.9 (d, ¹J = 13.7 Hz; CH_{COOD}), 69.8 (d, ¹J = 13.3 Hz; CH_{COOD}), 36.5, 32.4, 31.6, 28.5, 28.0 ppm; IR (KBr): $\tilde{\nu}$ = 2963.1, 2253.4, 1703.8, 1611.2, 1541.8, 1349.0, 1261.2, 1096.3, 801.3 cm⁻¹; HRMS (FAB): *m/z* calcd for C₁₈H₁₈ClN₆O₄Rh⁺: 520.0133 [*M*⁺]; found: 520.0130; elemental analysis calcd (%) for C₁₈H₁₈ClN₆O₄Rh: C 41.52, H 3.48, N 16.14; found: C 41.19, H 3.87, N 16.18.

Chloro(η⁴-cycloocta-1,5-diene)[2-(2,4-dinitrophenyl)-4-methyl-5-nitro-3H-1,2,4-triazol-3-ylidene]rhodium(I) (4c): A Schlenk tube (10 mL) wrapped in aluminium foil was charged with **3c**-HOTf (223 mg, 0.500 mmol), [[RhCl(cod)]₂] (123 mg, 0.250 mmol), K₂CO₃ (691 g, 5.00 mmol), and dry toluene (5 mL). The reaction mixture was stirred at room temperature for 3 d in the dark. After the reaction, the resulting salt and excess K₂CO₃ were filtered off, and the filtrate was concentrated under reduced pressure. The resulting solid was purified by column chromatography (SiO₂, CH₂Cl₂/acetone 50/1) and recrystallization from CH₂Cl₂/diethyl ether to give [RhCl(**3c**)(cod)] (**4c**) as an orange crystal (228 mg, 0.422 mmol, 84%). Single crystals suitable for X-ray diffraction analysis were obtained by slow diffusion of diethyl ether into a CH₂Cl₂ solution of **4c**. M.p. 207 °C (decomp); ¹H NMR (400.03 MHz, CDCl₃): δ = 9.46 (d, ³J = 8.7 Hz, 1H; CH_{6-Ar}), 8.95 (d, ⁴J = 2.5 Hz, 1H; CH_{3-Ar}), 8.79 (dd, ³J = 8.7, ⁴J = 2.5 Hz, 1H; CH_{5-Ar}), 5.34–5.20 (m, 2H; CH_{COOD}), 4.66 (s, 3H; CH₃), 3.57–3.50 (m, 1H; CH_{COOD}), 3.03–2.96 (m, 1H; CH_{COOD}), 2.52–2.37 (m, 2H; CH_{2COOD}), 2.14–1.77 (m, 5H; CH_{2COOD}), 1.72–1.58 ppm (m, 1H; CH_{2COOD}); ¹³C{¹H} NMR (100.60 MHz, [D₆]DMSO): δ = 198.1 (d, ¹J(Rh,C) = 53.5 Hz; NCN), 153.8, 148.0, 143.6, 135.0, 130.1, 128.1, 121.6, 101.3 (d, ¹J(Rh,C) = 6.6 Hz; CH_{COOD}), 101.1 (d, ¹J(Rh,C) = 6.5 Hz; CH_{COOD}), 70.0 (d, ¹J(Rh,C) = 14.0 Hz; CH_{COOD}), 69.9 (d, ¹J(Rh,C) = 13.6 Hz; CH_{COOD}), 38.7, 32.5, 31.5, 28.6, 27.9 ppm; IR (KBr): $\tilde{\nu}$ = 3053, 2877, 1608, 1578, 1544, 1345 cm⁻¹; HRMS (FAB): *m/z* calcd for C₁₇H₁₈ClN₆O₆Rh⁺: 540.0031 [*M*⁺]; found: 540.0019; elemental analysis calcd (%) for C₁₇H₁₈ClN₆O₆Rh: C 37.76, H 3.36, N 15.54; found: C 37.54, H 3.32, N 15.55.

Chlorodicarbonyl[2-(2,4-dinitrophenyl)-4-methyl-3H-1,2,4-triazol-3-ylidene]rhodium(I) (5a): CO gas was bubbled through a solution of **4a** (24.8 mg, 0.0500 mmol) in dry CH₂Cl₂ (5 mL) for IR analysis or in [D₆]acetone (1 mL) for NMR analysis at room temperature for 30 min. The initial brown solution became a light brown solution of [RhCl(**3a**)(CO)₂] (**5a**) (quantitative yield). The yield was determined by ¹H NMR spectroscopy based on COD. When the solution of **5a** was concentrated, **5a** decomposed. ¹H NMR (400.03 MHz, [D₆]acetone): δ = 9.01 (s, 1H; NCHN), 8.99 (d, ⁴J = 2.5 Hz, 1H; CH_{3-Ar}), 8.87 (dd, ³J = 8.7, ⁴J = 2.5 Hz, 1H; CH_{5-Ar}), 8.54 (d, ³J = 8.7 Hz, 1H; CH_{6-Ar}), 4.19 ppm (s, 3H; CH₃); ¹³C{¹H} NMR (100.60 MHz, [D₆]acetone): δ = 186.2 (d, ¹J(Rh,C) = 55.6 Hz; CO), 182.7 (d, ¹J(Rh,C) = 44.2 Hz; NCN), 182.2 (d, ¹J(Rh,C) = 76.0 Hz; CO), 149.3, 147.5, 146.0, 137.2, 132.8, 129.1, 122.1, 36.8 ppm; IR (CH₂Cl₂): $\tilde{\nu}$ = 2093.4 (CO), 2015.3 (CO), 1701.9 cm⁻¹; HRMS (ESI): *m/z* calcd for C₁₁H₇ClN₅NaO₆Rh + Na⁺: 465.90321 [*M* + Na⁺]; found: 465.90325.

Chlorodicarbonyl[5-cyano-2-(2,4-dinitrophenyl)-4-methyl-3H-1,2,4-triazol-3-ylidene]rhodium(I) (5b): CO gas was bubbled through a solution of **4a** (26.1 mg, 0.0500 mmol) in dry CH₂Cl₂ (5 mL) for IR analysis or in [D₆]acetone (1 mL) for NMR analysis at room temperature for 30 min. The initial orange solution became a yellow solution of [RhCl(**3b**)(CO)₂] (**5b**) (quantitative yield). The yield was determined by ¹H NMR spectroscopy based on COD. When the solution of **5b** was concentrated, **5b** decomposed. ¹H NMR (400.03 MHz, [D₆]acetone): δ = 9.08 (d, ⁴J = 2.5 Hz, 1H; CH_{3-Ar}), 8.92 (dd, ³J = 8.7, ⁴J = 2.5 Hz, 1H; CH_{5-Ar}), 8.47 (d, ³J = 8.7 Hz, 1H; CH_{6-Ar}), 4.39 ppm (s, 3H; CH₃); ¹³C{¹H} NMR (100.60 MHz, [D₆]acetone): δ = 186.9 (d, ¹J(Rh,C) = 45.2 Hz; NCN), 185.6 (d, ¹J(Rh,C) = 56.4 Hz; CO), 181.7 (d, ¹J = 71.7 Hz; CO), 150.1, 145.8, 136.2,

135.3, 133.5, 129.7, 122.5, 107.3, 37.8 ppm; IR (CH_2Cl_2): $\tilde{\nu}$ = 2099.1 (CO), 2021.0 cm^{-1} (CO); HRMS (ESI): m/z calcd for $\text{C}_{12}\text{H}_6\text{ClN}_6\text{NaO}_6\text{Rh} + \text{Na}^+$: 490.89846 [$M + \text{Na}^+$]; found: 490.89848.

Chlorodicarbonyl[2-(2,4-dinitrophenyl)-4-methyl-5-nitro-3H-1,2,4-triazol-3-ylidene]rhodium(I) (5c): CO gas was bubbled through a solution of **4c** (27.0 mg, 0.0500 mmol) in dry CH_2Cl_2 (5 mL) for IR analysis or in $[\text{D}_6]\text{acetone}$ (1 mL) for NMR analysis at room temperature for 30 min. The initial brown solution became a yellow solution of $[\text{RhCl}(\text{3c})(\text{CO})_2]$ (**5c**) (quantitative yield). The yield was determined by ^1H NMR spectroscopy based on COD. When the solution of **5c** was concentrated, **5c** decomposed. ^1H NMR (400.03 MHz, $[\text{D}_6]\text{acetone}$): δ = 9.11 (d, 4J = 2.5 Hz, 1H; $\text{CH}_{3-\text{Ar}}$), 8.94 (dd, 3J = 8.7, 4J = 2.5 Hz, 1H; $\text{CH}_{5-\text{Ar}}$), 8.47 (d, 3J = 8.7 Hz, 1H; $\text{CH}_{6-\text{Ar}}$), 4.56 ppm (s, 3H; CH_3); $^{13}\text{C}\{^1\text{H}\}$ NMR (100.60 MHz, $[\text{D}_6]\text{acetone}$): δ = 190.6 (d, $^1J(\text{Rh},\text{C})$ = 45.7 Hz; NCN), 185.7 (d, $^1J(\text{Rh},\text{C})$ = 56.1 Hz; CO), 181.7 (d, $^1J(\text{Rh},\text{C})$ = 71.9 Hz; CO), 150.2, 148.7, 145.8, 136.4, 133.8, 129.8, 122.6, 40.0 ppm; IR (CH_2Cl_2): $\tilde{\nu}$ = 3053.7, 2985.3, 2100.1 (CO), 2022.0 (CO), 1548.6, 1422.2, 1346.1, 895.8 cm^{-1} ; HRMS (ESI): m/z calcd for $\text{C}_{11}\text{H}_6\text{ClN}_6\text{NaO}_8\text{Rh} + \text{Na}^+$: 510.88829 [$M + \text{Na}^+$]; found: 510.88830.

Chloro[2-(2,4-dinitrophenyl)-4-methyl-3H-1,2,4-triazol-3-ylidene]gold(I) (6a): A Schlenk tube (10 mL) wrapped in aluminium foil was charged with **3a-HOTf** (1.20 g, 3.00 mmol), $\text{AuCl}(\text{SMe}_2)$ (884 mg, 3.00 mmol), K_2CO_3 (4.56 mg, 33.0 mmol), and dry toluene (30 mL). The reaction mixture was stirred at room temperature for 44 h in the dark. Then the resulting salt and excess K_2CO_3 were filtered off, and the solid was washed with hexane. The solid was suspended in acetone (30 mL). The solid was filtered off, and the filtrate was concentrated under reduced pressure. The resulting solid was washed with methanol (10 mL \times 3) and the solid was dried in vacuo to give $[\text{AuCl}(\text{3a})]$ (**6a**) as a white powder (453 mg, 0.941 mmol, 31%). Single crystals suitable for X-ray diffraction analysis were obtained by slow cooling of an acetone solution of **6a**. M.p. 201 °C (decomp); ^1H NMR (400.03 MHz, $[\text{D}_6]\text{DMSO}$): δ = 9.23 (s, 1H; NCHN), 8.97 (d, 4J = 2.5 Hz, 1H; $\text{CH}_{3-\text{Ar}}$), 8.82 (dd, 3J = 8.7, 4J = 2.5 Hz, 1H; $\text{CH}_{5-\text{Ar}}$), 8.40 (d, 3J = 8.7 Hz, 1H; $\text{CH}_{6-\text{Ar}}$), 3.95 ppm (s, 3H; CH_3); $^{13}\text{C}\{^1\text{H}\}$ NMR (100.60 MHz, $[\text{D}_6]\text{DMSO}$): δ = 175.1, 148.2, 146.5, 144.5, 135.0, 130.5, 129.1, 121.7, 35.9 ppm; IR (KBr): $\tilde{\nu}$ = 3144.4, 3094.2, 1613.2, 1544.7, 1349.9, 977.7, 854.3, 740.5 cm^{-1} ; HRMS (ESI): m/z calcd for $\text{C}_9\text{H}_7\text{N}_5\text{O}_4\text{AuCl} + \text{Na}^+$: 503.9750 [$M + \text{Na}^+$]; found: 503.9745; elemental analysis calcd (%) for $\text{C}_9\text{H}_7\text{AuClN}_5\text{O}_4$: C 22.45, H 1.47, N 14.54; found: C 22.73, H 1.76, N 14.28.

Chloro[2-(2,4-dinitrophenyl)-4-methyl-5-nitro-3H-1,2,4-triazol-3-ylidene]gold(I) (6c): A Schlenk tube (10 mL) wrapped in aluminium foil was charged with **3c-HOTf** (199 mg, 0.446 mmol), $\text{AuCl}(\text{SMe}_2)$ (132 mg, 0.446 mmol), K_2CO_3 (617 mg, 4.46 mmol), and dry toluene (10 mL). The reaction mixture was stirred at room temperature for 70 h in the dark. After the reaction, the resulting salt and excess K_2CO_3 were filtered off, and the solid was washed with hexane. Then, the solid was suspended in acetone (15 mL). The insoluble solid was filtered off, and the filtrate was concentrated under reduced pressure. The yellow solid was washed with methanol (5 mL \times 3) and dried in vacuo. The resulting solid was purified by recrystallization from acetone/hexane to give $[\text{AuCl}(\text{3c})]$ (**6c**) as a pale yellow crystal (114 mg, 0.216 mmol, 48%). Single crystals suitable for X-ray diffraction analysis were obtained by slow cooling of an acetone solution of **6c**. M.p. 205 °C (dec); ^1H NMR (400.03 MHz, $[\text{D}_6]\text{DMSO}$): δ = 9.04 (d, 4J = 2.5 Hz, 1H; $\text{CH}_{3-\text{Ar}}$), 8.86 (dd, 3J = 8.7, 4J = 2.5 Hz, 1H; $\text{CH}_{5-\text{Ar}}$), 8.34 (d, 3J = 8.7 Hz, 1H; $\text{CH}_{6-\text{Ar}}$), 4.22 ppm (s, 3H; CH_3); $^{13}\text{C}\{^1\text{H}\}$ NMR (100.60 MHz, $[\text{D}_6]\text{DMSO}$): δ = 181.5, 153.0, 148.9, 144.2, 133.9, 131.4, 129.8, 122.1, 30.7 ppm; IR (KBr): $\tilde{\nu}$ = 3115.4, 1611.2, 1582.3, 1540.8, 1458.9, 1441.5, 1347.0, 1331.6, 915.1, 848.5, 742.5 cm^{-1} ; HRMS (ESI): m/z calcd for $\text{C}_9\text{H}_6\text{N}_6\text{O}_6\text{AuCl} + \text{Na}^+$: 548.95951 [$M + \text{Na}^+$]; found: 548.95948; elemental analysis calcd (%) for $\text{C}_9\text{H}_6\text{AuClN}_6\text{O}_6$: C 20.53, H 1.15, N 15.96; found: C 20.89, H 1.28, N 15.73.

General procedure for Au-catalysed intermolecular hydroalkoxylation of cyclohexene (8) with 2-methoxyethanol (7): A septum-cap vial tube (2 mL) wrapped in aluminium foil was charged with Au complex (0.0125 mmol), AgNTE_2 (4.9 mg, 0.0125 mmol), and chlorobenzene (0.25 mL), and the mixture was stirred for 5 min. Cyclohexene (**8**, 205 mg, 2.50 mmol) and 2-methoxyethanol (**7**, 19.0 mg, 0.250 mmol) were

added to the mixture. The vial tube was sealed and stirred at 100 °C for 20 h. After the reaction, the mixture was cooled to room temperature. Then, *n*-tetradecane was added to the mixture as an internal standard. The yield of the resulting (2-methoxyethoxy)cyclohexane (**9**)^[15] was determined by GLC analysis.

General procedure for Au-catalysed intermolecular hydroalkoxylation of 1-octene with 1-octanol: A septum-cap vial tube (2 mL) wrapped in aluminium foil was charged with Au complex (0.0250 mmol), AgOTf (6.4 mg, 0.025 mmol), and benzotrifluoride (0.5 mL), and the mixture was stirred for 5 min. 1-Octene (561 mg, 5.00 mmol) and 1-octanol (65.1 mg, 0.500 mmol) were added to the mixture. The vial tube was sealed and stirred at 110 °C for 20 h. Then, the mixture was cooled to room temperature, and *n*-tetradecane was added to the mixture as an internal standard. The yields of the resulting 1-(octan-2-yloxy)octane^[21] and 1-(octyloxy)octane^[21] and molar ratios of products were determined by GLC analysis.

X-ray diffraction analysis: Single crystals coated with liquid paraffin were mounted on a thin nylon loop and fixed in a cold nitrogen stream. X-ray data were collected with a Bruker AXS APEX II CCD diffractometer using graphite-monochromated $\text{MoK}\alpha$ radiation (λ = 0.71073 Å). The data were corrected for Lorentzian and polarization effects. Data integration and reduction were performed with SAINT and XPREP software.^[22] Multiscan absorption corrections were applied by using the semiempirical method with SADABS.^[23] The structures were solved by direct methods with SHELXS-97^[24] and refined by full-matrix, least-squares methods on F^2 with SHELXL-97^[24] and Yadokari-XG 2009.^[25] Selected data and structure refinement for all relevant compounds are summarised in the Supporting Information (Tables S3–S5). CCDC 886836 (**3a-HOTf**), 886835 (**3b-HOTf**), 886837 (**3c-HOTf**), 886834 (**4a-acetonitrile**), 886832 (**4b**), 886833 (**4c**), 927996 (**6a-acetone**), and 895568 (**6c**) contain the supplementary crystallographic data for this paper. These data can be obtained free of charge from The Cambridge Crystallographic Data Centre via www.ccdc.cam.ac.uk/data_request/cif.

Computational analysis: All calculations were performed at the M06^[26]/cc-pVTZ^[27]/LanL2TZ(f)^[28](Rh) level with the Gaussian 09 program package^[29] and NBO analysis was carried out with the NBO version 3.1 program.^[30] For details of the calculations, see the Supporting Information.

Acknowledgements

This work was supported in part by a Grant-in-Aid for Scientific Research on Innovative Areas “Molecular Activation Directed toward Straightforward Synthesis” from MEXT, Japan and by a commissioned project conducted by New Energy and Industrial Technology Development Organization (NEDO). We thank Prof. K. Itaya (Tohoku University) for courteous permission to use the X-ray diffractometer and Dr. C. Kabuto (Tohoku University) for her kind advice in X-ray analysis. A part of the computational results were obtained using supercomputing resources at the Cyberscience Center, Tohoku University (Japan).

- [1] For selected general reviews, see: a) L. Benhamou, E. Chardon, G. Lavigne, S. Bellemin-Lapponnaz, V. César, *Chem. Rev.* **2011**, *111*, 2705–2733; b) T. Dröge, F. Glorius, *Angew. Chem.* **2010**, *122*, 7094–7107; *Angew. Chem. Int. Ed.* **2010**, *49*, 6940–6952; c) M. Melaimi, M. Soleilhavoup, G. Bertrand, *Angew. Chem.* **2010**, *122*, 8992–9032; *Angew. Chem. Int. Ed.* **2010**, *49*, 8810–8849; d) P. de Frémont, N. Marion, S. P. Nolan, *Coord. Chem. Rev.* **2009**, *253*, 862–892; e) O. Schuster, L. Yang, H. G. Raubenheimer, M. Albrecht, *Chem. Rev.* **2009**, *109*, 3445–3478; f) F. E. Hahn, M. C. Jahnke, *Angew. Chem.* **2008**, *120*, 3166–3216; *Angew. Chem. Int. Ed.* **2008**, *47*, 3122–3172; g) *N-Heterocyclic Carbenes in Transition Metal Catalysis* (Ed.: F. Glorius), Springer, Heidelberg, **2007**; h) *N-Heterocyclic Carbenes in Synthesis* (Ed.: S. P. Nolan) Wiley-VCH, Weinheim, **2006**; i) D. Bourissou, O. Guerret, F. P. Gabbaï, G. Bertrand, *Chem. Rev.* **2000**, *100*, 39–91; j) D. Martin, M. Melaimi, M. Soleilhavoup, G. Bertrand,

- Organometallics* **2011**, *30*, 5304–5313; For selected reviews on NHC–transition metal catalysis, see: k) S. Díez-González, N. Marion, S. P. Nolan, *Chem. Rev.* **2009**, *109*, 3612–3676; l) E. A. B. Kantchev, C. J. O'Brien, M. G. Organ, *Angew. Chem.* **2007**, *119*, 2824–2870; *Angew. Chem. Int. Ed.* **2007**, *46*, 2768–2813; m) F. Glorius, *Top. Organomet. Chem.* **2007**, *21*, 1–20; n) W. A. Herrmann, *Angew. Chem.* **2002**, *114*, 1342–1363; *Angew. Chem. Int. Ed.* **2002**, *41*, 1290–1309; For selected reviews on NHCs as organocatalysts, see: o) A. Grossmann, D. Enders, *Angew. Chem. Int. Ed.* **2012**, *51*, 314–325; p) J. L. Moore, T. Rovis, *Top. Curr. Chem.* **2010**, *291*, 118–144; q) V. Nair, S. Vellalath, B. P. Babu, *Chem. Soc. Rev.* **2008**, *37*, 2691–2698; r) D. Enders, O. Niemeier, A. Henseler, *Chem. Rev.* **2007**, *107*, 5606–5655; s) N. Marion, S. Díez-González, S. P. Nolan, *Angew. Chem.* **2007**, *119*, 3046–3058; *Angew. Chem. Int. Ed.* **2007**, *46*, 2988–3000.
- [2] a) M. D. Sanderson, J. W. Kamplain, C. W. Bielawski, *J. Am. Chem. Soc.* **2006**, *128*, 16514–16515; b) D. M. Khranov, V. M. Lynch, C. W. Bielawski, *Organometallics* **2007**, *26*, 6042–6049; c) A. G. Tennyson, R. J. Ono, T. W. Hudnall, D. M. Khranov, J. A. V. Er, J. W. Kamplain, V. M. Lynch, J. L. Sessler, C. W. Bielawski, *Chem. Eur. J.* **2010**, *16*, 304–315; d) V. César, N. Lugan, G. Lavigne, *Eur. J. Inorg. Chem.* **2010**, 361–365; e) M. Braun, W. Frank, G. J. Reiss, C. Ganter, *Organometallics* **2010**, *29*, 4418–4420; f) M. Braun, W. Frank, C. Ganter, *Organometallics* **2012**, *31*, 1927–1934; g) T. W. Hudnall, C. W. Bielawski, *J. Am. Chem. Soc.* **2009**, *131*, 16039–16041; h) V. César, N. Lugan, G. Lavigne, *Chem. Eur. J.* **2010**, *16*, 11432–11442; i) L. Benhamou, N. Vujkovic, V. César, H. Gornitzka, N. Lugan, G. Lavigne, *Organometallics* **2010**, *29*, 2616–2630; j) M. G. Hobbs, C. J. Knapp, P. T. Welsh, J. Borau-Garcia, T. Ziegler, R. Roesler, *Chem. Eur. J.* **2010**, *16*, 14520–14533; k) G. A. Blake, J. P. Moerdyk, C. W. Bielawski, *Organometallics* **2012**, *31*, 3373–3378; l) S. Saravanakumar, M. K. Kindermann, J. Heinicke, M. Köckerling, *Chem. Commun.* **2006**, 640–642; m) M. Alcarazo, R. Fernández, E. Álvarez, J. M. Lassaletta, *J. Organomet. Chem.* **2005**, *690*, 5979–5988; n) J. Iglesias-Sigüenza, A. Ros, E. Díez, M. Alcarazo, E. Álvarez, R. Fernández, J. M. Lassaletta, *Dalton Trans.* **2009**, 7113–7120; o) C. Dash, M. M. Shaikh, R. J. Butcher, P. Ghosh, *Inorg. Chem.* **2010**, *49*, 4972–4983; p) B. Hildebrandt, S. Raub, W. Frank, C. Ganter, *Chem. Eur. J.* **2012**, *18*, 6670–6678; q) G. D. Frey, V. Lavallo, B. Donnadiou, W. W. Schoeller, G. Bertrand, *Science* **2007**, *316*, 439–441; r) S. Fantasia, J. L. Petersen, H. Jacobsen, L. Cavallo, S. P. Nolan, *Organometallics* **2007**, *26*, 5880–5889; s) O. Back, M. Henry-Ellinger, C. D. Martin, D. Martin, G. Bertrand, *Angew. Chem. Int. Ed.* **2013**, *52*, 2939–2943; t) V. Lavallo, Y. Canac, B. Donnadiou, W. W. Schoeller, G. Bertrand, *Angew. Chem.* **2006**, *118*, 3568–3571; *Angew. Chem. Int. Ed.* **2006**, *45*, 3488–3491.
- [3] T. Sato, Y. Hirose, D. Yoshioka, S. Oi, *Organometallics* **2012**, *31*, 6995–7003.
- [4] a) W. A. Herrmann, J. Schütz, G. D. Frey, E. Herdtweck, *Organometallics* **2006**, *25*, 2437–2448; b) G. S. Nichol, J. Rajaseelan, L. J. Anna, E. Rajaseelan, *Eur. J. Inorg. Chem.* **2009**, 4320–4328; c) R. B. Strand, T. Helgerud, T. Solvang, A. Dolva, C. A. Sperger, A. Fiksdahl, *Tetrahedron: Asymmetry* **2012**, *23*, 1350–1359; d) R. B. Strand, T. Solvang, C. A. Sperger, A. Fiksdahl, *Tetrahedron: Asymmetry* **2012**, *23*, 838–842; e) A. Ros, M. Alcarazo, J. Iglesias-Sigüenza, E. Díez, E. Álvarez, R. Fernández, J. M. Lassaletta, *Organometallics* **2008**, *27*, 4555–4564; f) J. Francos, F. Grande-Carmona, H. Faustino, J. Iglesias-Sigüenza, E. Díez, I. Alonso, R. Fernández, J. M. Lassaletta, F. López, J. L. Mascareñas, *J. Am. Chem. Soc.* **2012**, *134*, 14322–14325; g) S. Paul, W. B. Schweizer, M.-O. Ebert, R. Gilmour, *Organometallics* **2010**, *29*, 4424–4427.
- [5] M. Alcarazo, T. Stork, A. Anoop, W. Thiel, A. Fürstner, *Angew. Chem.* **2010**, *122*, 2596–2600; *Angew. Chem. Int. Ed.* **2010**, *49*, 2542–2546.
- [6] For details of characterisation, see the Supporting Information.
- [7] X.-Y. Yu, B. O. Patrick, B. R. James, *Organometallics* **2006**, *25*, 2359–2363.
- [8] X.-Y. Yu, H. Sun, B. O. Patrick, B. R. James, *Eur. J. Inorg. Chem.* **2009**, 1752–1758.
- [9] a) C. A. Tolman, *J. Am. Chem. Soc.* **1970**, *92*, 2953–2965; b) C. A. Tolman, *Chem. Rev.* **1977**, *77*, 313–348.
- [10] a) R. A. Kelly III, H. Clavier, S. Giudice, N. M. Scott, E. D. Stevens, J. Bordner, I. Samardjiev, C. D. Hoff, L. Cavallo, S. P. Nolan, *Organometallics* **2008**, *27*, 202–210; b) S. Wolf, H. Plenio, *J. Organomet. Chem.* **2009**, *694*, 1487–1492.
- [11] The order of the values of $\tilde{\nu}_{av}(\text{CO})$, that is, the order of the TEP values, necessarily corresponds to the ^{13}C NMR shift of the carbenic carbon atoms. For example, see ref. [4a].
- [12] S. I. Lee, S. Y. Park, J. H. Park, I. G. Jung, S. Y. Choi, Y. K. Chung, B. Y. Lee, *J. Org. Chem.* **2006**, *71*, 91–96.
- [13] The % V_{bur} value is a measure of the steric bulk of a ligand. The % V_{bur} values were calculated from the corresponding crystallographic data by using the SambVca program. For the SambVca program, see: a) A. Poater, B. Cosenza, A. Correa, S. Giudice, F. Ragone, V. Scarano, L. Cavallo, *Eur. J. Inorg. Chem.* **2009**, 1759–1766; b) <http://www.molnac.unisa.it/OMtools.php>.
- [14] R. H. Crabtree, J. M. Quirk, *J. Organomet. Chem.* **1980**, *199*, 99–106.
- [15] T. Hirai, A. Hamasaki, A. Nakamura, M. Tokunaga, *Org. Lett.* **2009**, *11*, 5510–5513.
- [16] W. Wang, G. B. Hammond, C. Xu, *J. Am. Chem. Soc.* **2012**, *134*, 5697–5705.
- [17] J. H. Teles, S. Brode, M. Chabanas, *Angew. Chem.* **1998**, *110*, 1475–1478; *Angew. Chem. Int. Ed.* **1998**, *37*, 1415–1418.
- [18] For details of calculations, see the Supporting Information (Tables S9 and S10).
- [19] J. F. K. Wilshire, *Aust. J. Chem.* **1966**, *19*, 1935–1945.
- [20] K. Walczak, A. Gondele, J. Suwiński, *Eur. J. Med. Chem.* **2004**, *39*, 849–853.
- [21] Y. Fujii, H. Furugaki, E. Tamura, S. Yano, K. Kita, *Bull. Chem. Soc. Jpn.* **2005**, *78*, 456–463.
- [22] SMART, SAINT and XPREP, Bruker Analytical X-ray Instruments Inc: Madison, WI, USA, **1995**.
- [23] G. M. Sheldrick, SADABS, Empirical Absorption Correction Program for Area Detector Data, University of Göttingen, Göttingen (Germany), **1996**.
- [24] G. M. Sheldrick, SHELEX-97, Programs for the Refinement of Crystal structures, University of Göttingen, Göttingen (Germany), **1997**.
- [25] a) K. Wakita, Yadokari-XG, Software for Crystal Structure Analyses, **2001**; b) C. Kabuto, S. Akine, T. Nemoto, E. Kwon, *J. Cryst. Soc. Jpn.* **2009**, *51*, 218–224.
- [26] Y. Zhao, D. G. Truhlar, *Theor. Chem. Acc.* **2008**, *120*, 215–241.
- [27] R. A. Kendall, T. H. Dunning, R. J. Harrison, *J. Chem. Phys.* **1992**, *96*, 6796–6806.
- [28] a) L. E. Roy, P. J. Hay, R. L. Martin, *J. Chem. Theory Comput.* **2008**, *4*, 1029–1031; b) P. J. Hay, W. R. Wadt, *J. Chem. Phys.* **1985**, *82*, 299–310.
- [29] Gaussian 09, Revision C.01, M. J. Frisch, G. W. Trucks, H. B. Schlegel, G. E. Scuseria, M. A. Robb, J. R. Cheeseman, G. Scalmani, V. Barone, B. Mennucci, G. A. Petersson, H. Nakatsuji, M. Caricato, X. Li, H. P. Hratchian, A. F. Izmaylov, J. Bloino, G. Zheng, J. L. Sonnenberg, M. Hada, M. Ehara, K. Toyota, R. Fukuda, J. Hasegawa, M. Ishida, T. Nakajima, Y. Honda, O. Kitao, H. Nakai, T. Vreven, J. A. Montgomery, Jr., J. E. Peralta, F. Ogliaro, M. Bearpark, J. J. Heyd, E. Brothers, K. N. Kudin, V. N. Staroverov, R. Kobayashi, J. Normand, K. Raghavachari, A. Rendell, J. C. Burant, S. S. Iyengar, J. Tomasi, M. Cossi, N. Rega, J. M. Millam, M. Klene, J. E. Knox, J. B. Cross, V. Bakken, C. Adamo, J. Jaramillo, R. Gomperts, R. E. Stratmann, O. Yazyev, A. J. Austin, R. Cammi, C. Pomelli, J. W. Ochterski, R. L. Martin, K. Morokuma, V. G. Zakrzewski, G. A. Voth, P. Salvador, J. J. Dannenberg, S. Dapprich, A. D. Daniels, Ö. Farkas, J. B. Foresman, J. V. Ortiz, J. Cioslowski, D. J. Fox, Gaussian, Inc., Wallingford, CT, **2009**.
- [30] E. D. Glendening, A. E. Reed, J. E. Carpenter, F. Weinhold, *NBO Version 3.1*.

Received: July 3, 2013
Published online: October 8, 2013